An Enhanced Analysis of Inter-Laminar Faults in Magnetic Cores with Grain Oriented Electrical Steels for Fault Diagnosis and Condition Monitoring: Theoretical Background and Experimental Verification

Hamed Hamzehbahmani, *Senior member, IEEE*

Abstract- **Fault diagnosis and condition monitoring of electromagnetic devices are the strategies of monitoring and processing parameters of the device for fault identification and failure prediction. In this respect, core faults or inter-laminar faults (ILFs) is a key objective, with an important contribution into the whole process. This paper tends to propose a new experimental-analytical approach to fault diagnosis and condition monitoring of magnetic cores. The proposed technique is in line with the phenomenology of the magnetic hysteresis and interpreting dynamic characteristics of the magnetic cores. The distinct feature of this approach is its ability to model additional magnetic field and associated energy loss caused by ILFs. The studies were carried out on stacks of standard Epstein size strips of 3 wt % SiFe Grain Oriented (GO) steels, subjected to artificial faults. Validation of the developed approach was undertaken through experimental work and analytical modelling.**

Index Terms- **Fault diagnosis, condition monitoring, transformer core, magnetic loss, grain oriented electrical steel, dynamic hysteresis loop, dynamic modelling.**

NOMENCLATURE

W_{tot}	Total energy loss
W_{hys}	Hysteresis energy loss
W_{eddy}	Classical eddy current energy loss
W_{exc}	Excess energy loss
$H(t)$	Magnetic field at the surface of the lamination
$H_{hys}(t)$	Hysteresis field
$H_{eddy}(t)$	Eddy current field
$H_{exc}(t)$	Excess field
W_{dyn}	Dynamic energy loss
$H_{dyn}(t)$	Dynamic field
$g_{dyn}(B)$	Polynomial function to control shape of DHL
δ	Directional parameter
α_{dyn}	Variable to determine frequency law of W_{exc}
W_{add}	Additional energy loss
$H_{add}(t)$	Additional field
$k_{add}(B)$	Polynomial function to control shape of DHL
B_m	Peak flux density
H_m	Peak magnetic field
H_b	Magnetic field at B_m
ΔH_a	Magnetic field on ascending branch
ΔH_d	Magnetic field on descending branch
μ_r	Relative permeability
P	Localised power loss
T	Localised temperature
c_p	Specific heat of the material

I. INTRODUCTION

Condition monitoring of electromagnetic devices, e.g. electrical machines and power transformers, is a procedure to monitor operational parameters of the device to detect and identify any faults at an early stage. Fault diagnosis can be performed by monitoring certain parameters and interpreting their physical characteristics to predict and identify faults in a timely manner [1-3]. Timely and reliable fault diagnosis not only prevents premature failure of the devices but helps to increase the reliability of the power systems. Power transformers are key components of the power systems with a major function of voltage conversion and power transfer between different parts of the power systems. With the continues development of power systems and electric networks, fault diagnosis and condition monitoring of power transformers become more important than ever. The importance of timely fault diagnosis of power transformers, and other electromagnetic devices, is more significant for grid connected renewable energy systems and smart grids.

Faults in power transformers can be generally categorised into external and internal faults. External faults occur due to external reasons, e.g. overvoltage caused by lightning strike, and overcurrent caused by external short circuits. Internal faults, on the other hand could happen due to internal reasons, for example failures in the electrical windings, magnetic core, tap changer, bushings and terminals. Statistical data show that 70 to 80 % of failures in power transformers arise from the internal faults [4]. Electrical windings and magnetic cores, as the main parts of all types of power transformers, are subjected to variety of different types of faults. Therefore, specific attentions have been drawn to their quality and conditions during the lifetime of the devices. The primary concern of this paper is to study core faults in electromagnetic devices constructed from Grain Oriented (GO) electrical steels, such as power transformers.

Magnetic core of electromagnetic devices is a laminated structure which make them vulnerable to faults. These kinds of faults are classified as core faults or inter-laminar faults (ILFs). Core faults principally arise from the laminated structure of the

magnetic cores. ILFs problem could emerge during the manufacturing processes of the magnetic cores, as well as during the operation and lifetime of the devices [5-7]. ILFs and their consequences have been addressed as a momentous threat to normal operation of all kinds of electromagnetic devices with laminated core. ILFs may cause fault current loops in the cores, which could result in inter-laminar fault currents between the neighbouring laminations. Localised power loss and temperature are the main consequences of core faults. If ILFs are not identified and detected in a timely manner, they could likely spread to the adjacent laminations due to severe local hot spots, and potentially lead to irreversible failure of the magnetic cores and the devices. An example of core failure at the T-joint of a three-phase distribution transformer is shown in Fig 1.
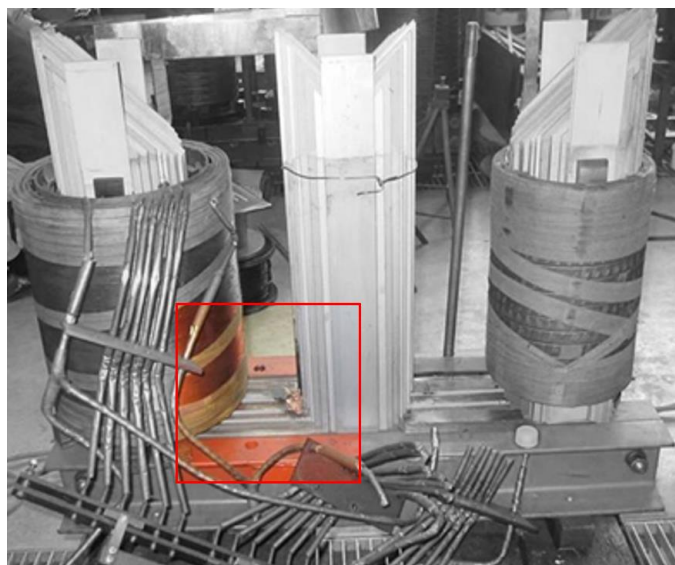
(a)

(b)

Fig 1 Core failure on T-joint of a three-phase distribution transformer

Following decades of research and development, all aspects and concepts of ILFs and their consequences on the magnetic cores are fully understood for the design and operation engineers [8-10]. Therefore, to prevent irreversible failures and breakdowns of the device, it is widely acknowledged that fault diagnosis of magnetic cores should be conducted at an early stage. Practical techniques have been developed and commercialized for fault diagnosis and condition monitoring of magnetic cores of all types of electromagnetic devices. In all of these techniques, practical data are acquired from measurement after magnetising the magnetic core. The measured parameters could be magnetic field, power loss, temperature, etc. The acquired data are then processed and translated into information to monitor status of the concerned magnetic core, which is in line with the principle and definition of condition monitoring [4]. Advanced data analysis and signal processing approaches, e.g. Artificial Neural Network (ANN) and Artificial Intelligence (AI), have been recently implemented for accurate fault diagnosis of all types of electromagnetic devices [11-12].

Historical development of the practical techniques of core quality assessment and fault diagnosis is appreciably reviewed in the literatures [13-15]. Most of the existing techniques are mainly developed for stator cores of turbo generators. Nevertheless, they can be further evolved and implemented for power transformers [16-18]. Core quality assessment of power transformers is mainly performed by measuring overall power losses of the core, known as no-load losses, as defined by the British standard BS EN 60076-1-2011 [19]. Measurement of no-load losses is performed after assembling the transformer at the manufacturer site, and during the routine and type tests. This however does not provide a realistic image of quality of the magnetic core, because it only gives overall power losses of the magnetic core. In recent studies conducted by the author [10], [20, 21], it was analytically and experimentally demonstrated that phenomenology of magnetic hysteresis is a reliable approach for fault diagnosis of magnetic cores. This could be accomplished effectively through examining the dynamic characteristics of the magnetic cores based on the instantaneous waveforms of the total magnetic field and its components, as well as the measured dynamic hysteresis loops (DHLs).

The original contribution of this paper is to perform advanced analytical and experimental studies to identify energy loss mechanism of magnetic cores, subjected to ILFs. In this respect, artificial short circuits faults of different configurations were introduced between stacks of four standard Epstein size laminations. Static Hysteresis Loop (SHL) of the test samples were initially constructed to identify static hysteresis energy loss of the test samples. Analytical modelling, based on the statistical energy loss principle, was then performed to calculate the additional magnetic field and associated energy loss. With the proposed technique, important quantities of the test samples including SHL, DHL, relative permeability, instantaneous waveforms of magnetic field strength $H(t)$, and more importantly additional magnetic field and associated energy loss caused by ILFs can be effectively monitored. Analysing these parameters can provide a proper image on quality of the concerned magnetic core. The developed approach provides further insight on dynamic behaviour and more importantly energy loss mechanism of the magnetic cores, when subjected to ILFs. This can provide a platform for fault diagnosis and condition monitoring of laminated magnetic cores, by measuring and interpreting the hysteresis loops. As a supplementary task, a thermometric method was used to measure localised power loss of the test samples based on the initial rate of rise of temperature method.

II. THEORETICAL BACKGROUND

Magnetising process and energy loss mechanism of the magnetic materials and magnetic cores can be examined, with high accuracy, through the hysteresis phenomenon. Accurate figures of the static and dynamic hysteresis loops of the magnetic materials have been adopted as a reliable technique to understand the materials behaviour and energy loss mechanism. The main role of the magnetic materials is to create a magnetic circuit for magnetic flux in the electromagnetic devices. However, their characteristics and behaviours are different, which mainly depend on their grain and domain structure, and crystallographic texture. Therefore, different analytical tools have been adopted to analyse their magnetic behaviour, energy loss mechanism and energy loss components.

A. Energy loss mechanism of GO steels:

GO electrical steels are the core materials for the power transformers, reactors, and large turbogenerators. Due to the anisotropic texture and grain structure of the material, it is widely admitted that dynamic behaviour of GO electrical steels can be adequately studied based on the Thin Sheet Model (TSM) originated from the statistical energy loss separation principle developed by Bertotti [22]. In this method, the total energy loss W_{tot} is separated into hysteresis loss W_{hys}, classical eddy current loss W_{eddy}, and excess loss W_{exc} [23]:

$$W_{tot} = W_{hys} + W_{eddy} + W_{exc} \qquad (1)$$

Energy loss mechanism can be analysed by interpreting the static and dynamic hysteresis loops for one magnetising cycle, for each particular frequency and flux density. Therefore, (1) can be converted into magnetic field separation [23]:

$$H(t) = H_{hys}(t) + H_{eddy}(t) + H_{exc}(t) \qquad (2)$$

where $H(t)$ is the magnetic field at the surface of the lamination, $H_{hys}(t)$ is hysteresis field, $H_{eddy}(t)$ is eddy current field, and $H_{exc}(t)$ is excess field. It should be noted that, using the three components loss model (2) under complex magnetisation conditions does not necessarily yield a realistic figure of energy loss mechanism of the materials. Non-sinusoidal magnetisation [24] and magnetic cores subjected to ILFs [20] are examples where the materials experience complex magnetisation regimes. In these cases, it is more convenience to use a two components loss model, where the total energy loss and total magnetic field are separated into hysteresis and dynamic components [24]:

$$W_{tot} = W_{hys} + W_{dyn} \qquad (3)$$

$$H(t) = H_{hys}(t) + H_{dyn}(t) \qquad (4)$$

A dynamic model for GO materials based on the two terms energy loss is proposed in [24]:

$$H(t) = H_{hys}(B(t)) + g_{dyn}(B)\delta \left|\frac{dB}{dt}\right|^{\alpha_{dyn}(B_{pk})} \qquad (5)$$

where $\delta = sign(dB/dt)$ is a directional parameter for ascending ($dB/dt > 0$) and descending ($dB/dt < 0$) branches

of the hysteresis loop. The exponent $\alpha_{dyn}(B_{pk})$ determines the frequency law of the excess loss component, and $g_{dyn}(B)$, in general, is a polynomial function which control shape of the constructed DHL [23, 25].

The two components TSM (5) shows that hysteresis field $H_{hys}(B(t))$ and hysteresis energy loss are rate-independent, while the dynamic magnetic field $H_{dyn}(t)$ and dynamic energy loss are rate-dependent. On other word, hysteresis energy loss is independent from the magnetising frequency, but dynamic energy loss increases by increasing the magnetising frequency. This is an important feature of the magnetising process and energy loss mechanism of the material. Accuracy of TSM (5) in characterising GO electrical steels and energy loss analysis has been proved in the recent publications [20, 24].

B. Energy loss mechanism of magnetic cores subjected to ILFs:

In the recent publications it was experimentally showed that dynamic characteristics of the magnetic cores are severely deteriorated when subjected to ILFs [20, 21]. This implies that impacts of ILFs on magnetic characteristics and magnetising processes of the magnetic cores are purely rate dependent. Therefore, the two terms TSM (5) was found as a reliable base to evaluate impacts of the ILFs on dynamic performance of the magnetic cores and energy loss analysis [20]. The first and immediate impact of ILFs is to create additional eddy current loops within the defected laminations, which result in additional localised power loss at the defected zone. A perspective view of a stack of laminations with ILF, and corresponding eddy current loops are schematically shown in Figs 2-a and 2-b, respectively.
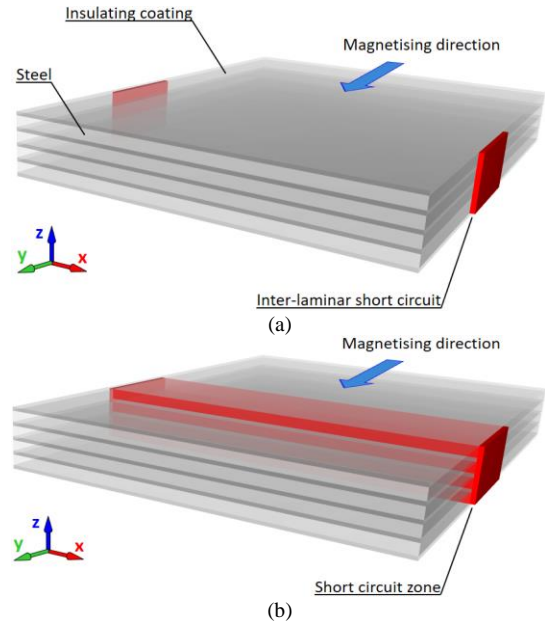

Fig 2 Influence of ILFs in magnetic core (a) stack of laminations with ILF, (b) corresponding eddy current path (not to scale)

The circulating eddy currents demand for additional magnetic field strength which contribute to the additional localised and overall power losses in the core. Therefore, in this work the two components TSM (5) was further developed to represent the additional loss and additional magnetic field caused by ILFs:

$$W_{tot} = W_{hys} + W_{dyn} + W_{add} \qquad (6)$$

$$H(t) = H_{hys}(B) + H_{dyn}(t) + H_{add}(t) \qquad (7)$$

where W_{add} and $H_{add}(t)$ are additional energy loss and additional magnetic field caused by the ILFs. Considering the hysteresis magnetic field and dynamic magnetic field of the two terms TSM as the basis of this modelling, (7) yields:

$$H(t) = H_{hys}(B) + g_{dyn}(B)\delta \left|\frac{dB}{dt}\right|^{\alpha_{dyn}(B_{pk})} + k_{add}(B)\frac{dB}{dt} \qquad (8)$$

Similar to $g_{dyn}(B)$, $k_{add}(B)$ is a polynomial function of the flux density B to control overall shape of the DHL.

III. Experimental set-up

Experimental works were performed on 0.3 mm thick standard Epstein size laminations of 3 % SiFe GO steels, with a resistivity of $\rho = 0.461\ \mu\Omega\text{m}$. Three stacks, each contains four strips, were assembled and marked as: Stack # 1 with no ILF, Stack # 2 with ILFs at one position, and Stack # 3 with ILFs at three positions. Following the previous work [20, 21], artificial faults were introduced on sides of the stacks using lead-free solder. Fig 3 shows a perspective view of the test samples.

(a)

(b)

(c)
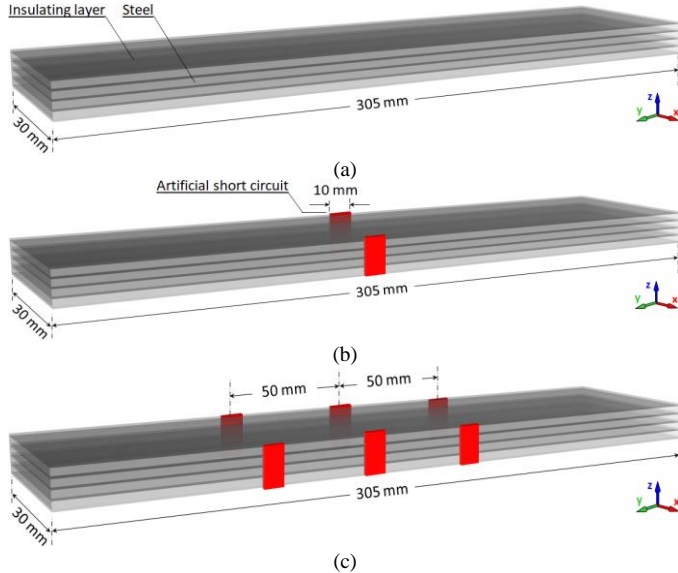
Fig 3 Perspective view of the test samples,
(a) Stack #1, (b) Stack #2 and (c) Stack #3 (not to scale)

A computer-controlled magnetising system based on single strip tester (SST) was used to magnetise the test samples [15], which is in line with the British standard BS EN 10280:2007 [26]. According to the guidance provided in UKAS M3003 [27], an in-depth uncertainty analysis of the measuring system was carried out. In this respect, Type A and Type B uncertainties were estimated at ± 0.30 % and ± 0.63 %, respectively.

IV. Experimental Verification and Analytical Modelling

According to the TSMs (5) and (8), dynamic hysteresis modelling starts with the hysteresis field component

$H_{hys}(B(t))$. Hysteresis field may be calculated using a reliable static or quasi-static hysteresis model. Therefore, the first step in modelling the DHL and magnetising process is to formulate the static hysteresis loop (SHL). Modelling process is then completed by adding other two field components, dynamic magnetic field $H_{dyn}(t)$ and additional magnetic field $H_{add}(t)$.

A. Magnetising processes and constructing the SHL:

In a recent publication it was experimentally demonstrated that monitoring the DHLs of ferromagnetic materials for a range of flux densities, from zero to the saturation level, allows the construction of the SHL with a great accuracy [28]. The proposed technique employs the phenomenological concepts of rate-dependent and rate-independent energy loss components under time varying magnetic field. In general, when ferromagnetic materials are subjected to time varying magnetic fields, two salient points can be underlined on the DHL during each magnetising cycle. (B_m, H_m) where the instantaneous wave shapes of flux density $B(t)$ and magnetic field strength $H(t)$ reach the maximum values, and (B_m, H_b) where the flux density changes its direction and $dB/dt = 0$.

Following the proposed approach in [28], DHLs of the samples were measured at peak flux densities from 0.1 T to 1.7 T and a frequency of 50 Hz. (B_m, H_m) and (B_m, H_b) curves were identified for the range of measured flux density; the results are shown in Fig 4. It is clear that, (B_m, H_b) curves for Stacks # 2 and # 3, with artificial faults, fairly coincide with that of Stack # 1. However, a significant deviation between the (B_m, H_m) of Stacks # 2 and # 3 with reference to that of Stack # 1 can be observed. On other word, Fig 4 shows that magnetic field strength H_b of the test samples is correlated with the peak flux density B_m for the measured range of flux density. In contrast, peak magnetic field strength H_m increases with increase in the number of the ILFs. An in-depth analysis on these two curves can provide an insight on impacts of ILFs on overall properties of the magnetic cores, magnetising processes, and energy loss mechanism. According to the general concept of the magnetic hysteresis, relative permeability μ_r of ferromagnetic materials can be calculated by tracking down the (B_m, H_m) curve. Based on the experimental results of Fig 4, relative permeability of the test samples was determined for the measured range of flux density; the results are shown in Fig 5.

It is evidence from Fig 5 that μ_r of the test samples are dramatically declined when subjected to ILFs. This phenomenon is more pronounced for the middle range flux densities, $1.0\ T \leq B_m \leq 1.5\ T$, where H_b is deviated from H_m. This experiment explicitly reveals that ILFs have a profound impact on the permeability of magnetic cores, which directly influence the overall quality of the device. Nevertheless, they may not necessarily degrade the intrinsic properties of the materials, e.g. relative permeability and specific power loss [10].
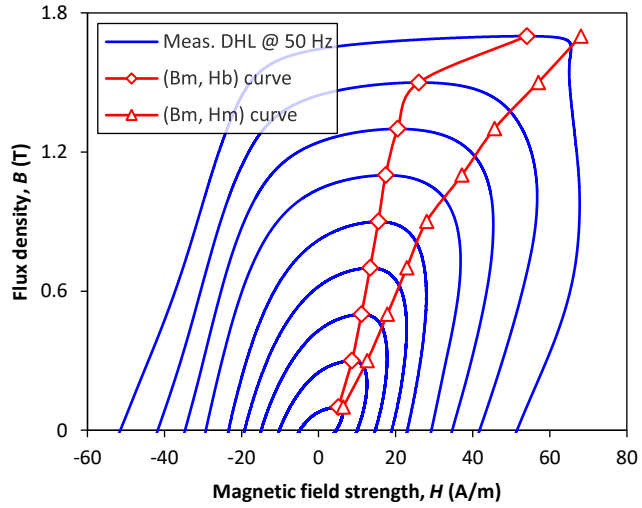
More details of the magnetic characteristics of the material can be acquired from the (B_m, H_b) curve, which can be used to analyse the energy loss mechanism and magnetising processes. Significance of the (B_m, H_b) curve in magnetic hysteresis can be evidenced based on the phenomenological concepts of rate-dependent and rate-independent energy loss components.
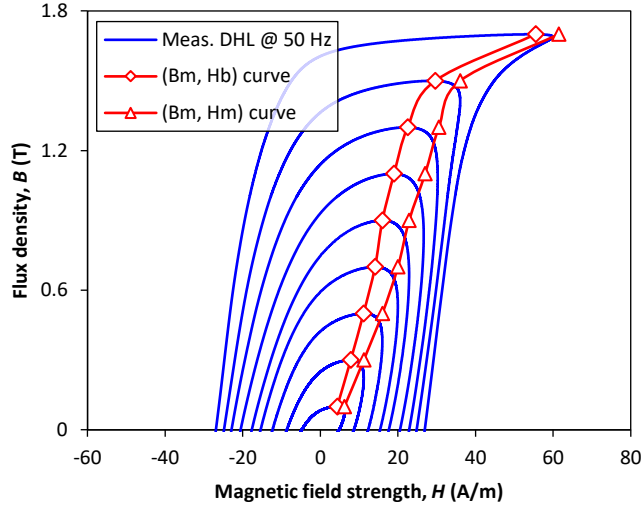
(a)
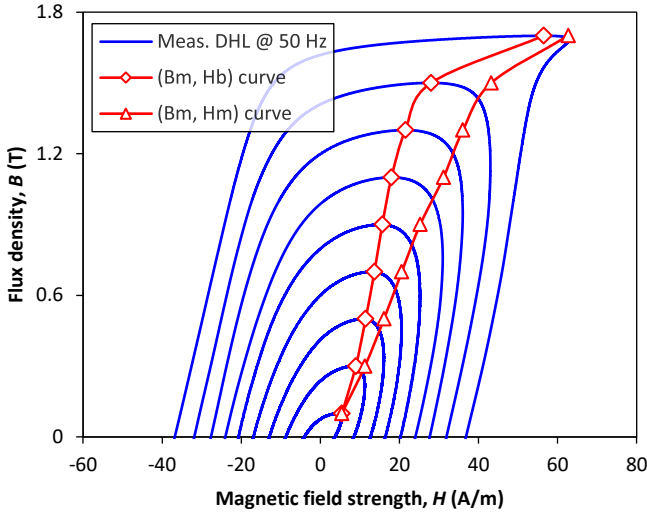
(b)

(c)

Fig 4 Dynamic hysteresis loops and corresponding (B_m, H_b) and (B_m, H_m) curves at $f = 50\ Hz$ and $B_{pk} = 1.1\ T$ to $B_{pk} = 1.7\ T$
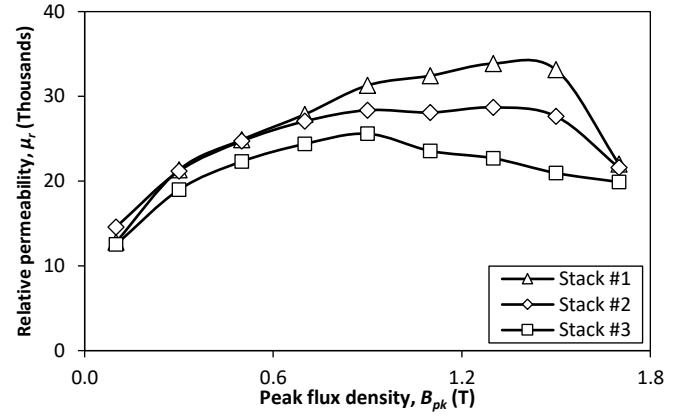(a) Stack #1 (b) Stack #2, and (c) Stack #3

Fig 5 Relative permeability measured from the (B_m, H_m) curve at $f = 50\ Hz$

TSM (5) shows that at $(B_m,\ H_b)$ where $dB/dt = 0$, dynamic magnetic field $H_{dyn}(t)$ is vanished, and total magnetic field $H(t)$ is exclusively equal to the hysteresis field $H_{hys}(B(t))$. Similar conclusion can be conducted from model (8) for a stack of laminations subjected to ILF. As a phenomenological result, ascending branch of the SHL can be constructed from the (B_m, H_b) datapoints, which is the first step to construct the SHL.

According to the TSMs (5) and (8), rate of dB/dt increases by increasing the magnetising frequency. Magnetic hysteresis responds to this by widening the loop area. Therefore, at a particular frequency, the instantaneous value of the ascending branch of the DHL can be expressed as follows:

$$H_a(B(t)) = H_{hys}(B(t)) + \Delta H_a \qquad (9)$$

where ΔH_a is the magnetic field strength corresponding to the dynamic energy loss component on the ascending branch.

At $(B_m,\ H_b)$ where dB/dt changes its direction, DHL spins to the descending branch. According to the TSMs (5) and (8) magnetic hysteresis pursues the same dynamic as for the ascending branch to build the descending branch of the DHL. Therefore, (9) can be also used to show the relationship between the SHL and DHL on the descending branch:

$$H_d(B(t)) = H_{hys}(B(t)) + \Delta H_d \qquad (10)$$

$H_a(B(t))$ and $H_d(B(t))$ are the instantaneous values of the ascending and descending branches of the DHL and can be measured at a low frequency. In this work, these data were acquired at frequency of 50 Hz. Accordingly, SHL of the test samples were constructed; the results at peak flux densities of 1.1 T to 1.7 T are shown in Fig 6.

B. Dynamic modelling and dynamic characteristics:

Dynamic characteristics of the test samples, including the instantaneous waveforms of the magnetic field strength and DHLs, were reproduced using the TSM (5) and (8). Following a recent work [20], a constant exponent of $\alpha_{dyn}(B_{pk}) = 0.57$ was found adequate for the measured range of flux density, and all test samples. Dynamic modelling of Stack # 1 was performed based on the two terms TSM (5), which is similar to that for a single strip. The following function for $g_{dyn}(B)$ was found acceptable to represent $H_{dyn}(t)$ of Stack # 1 at $B_{pk} = 1.7\ T$:
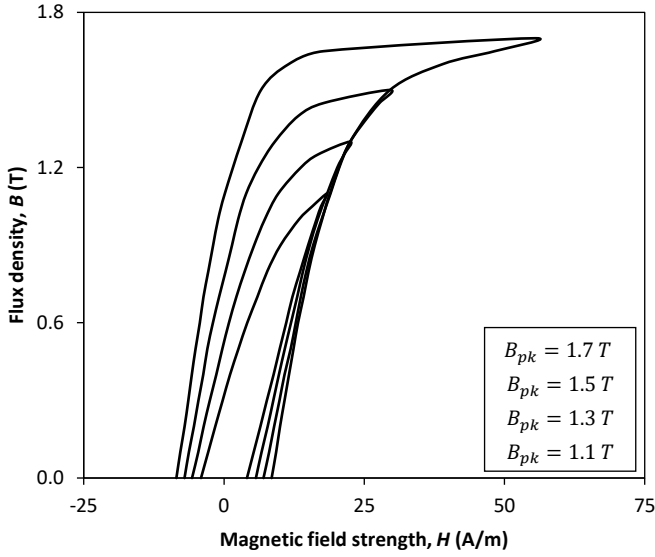
5

Fig 6 Constructed SHL of the test samples at $B_{pk} = 1.1\,T$ to $B_{pk} = 1.7\,T$

$$g_{dyn1}(B) = \begin{cases} 0.51(1 + 0.1\,B^2) & -1.7 < B < 1.4 \\ 0.66 & 1.4 < B < 1.7 \end{cases} \quad (11)$$

Dynamic modelling of Stacks # 2 and # 3, on the other hand, was performed based on the TSM (8). Additional filed $H_{add}(t)$ was calculated for each test sample and each flux density, to represent impact of the ILFs on the dynamic behaviour of the test samples. Computational functions that have been designated for $k_{add}(B)$ for Stack # 2 and Stack # 3 at $B_{pk} = 1.7\,T$, are given in (12) and (13), respectively:

$$k_{add2}(B) = \begin{cases} -0.74 - 0.34B(B - 3) & -1.7 < B < -1.3 \\ 0.02 + 0.011B(B - 1.78) & -1.3 < B < 0 \\ 0.013B + 0.019 & 0 < B < 1.7 \end{cases}$$
$$(12)$$

$$k_{add3}(B) =$$
$$\begin{cases} 0.343 + 0.19B(B - 2.57) & -1.7 < B < -1.4 \\ 0.047 + 0.023B(B - 1.87) & -1.4 < B < 0 \\ 0.045 - 0.015B(B - 3.12) & 0 < B < 1.3 \\ -0.408 - 0.23B(B - 2.93) & 1.3 < B < 1.7 \end{cases}$$
$$(13)$$

Fig 7 compares the measured and modelled DHLs for the measured range of flux density and frequency. In this modelling, the hysteresis magnetic field $H_{hys}(B)$ was represented using the constructed SHLs of Fig 6. The instantaneous waveforms of the total magnetic field $H(t)$, and additional magnetic field $H_{add}(t)$ for one magnetising cycle at peak flux densities of $B_{pk} = 1.1$ T to $B_{pk} = 1.7$ T are shown in Figs 8 to 11, respectively.
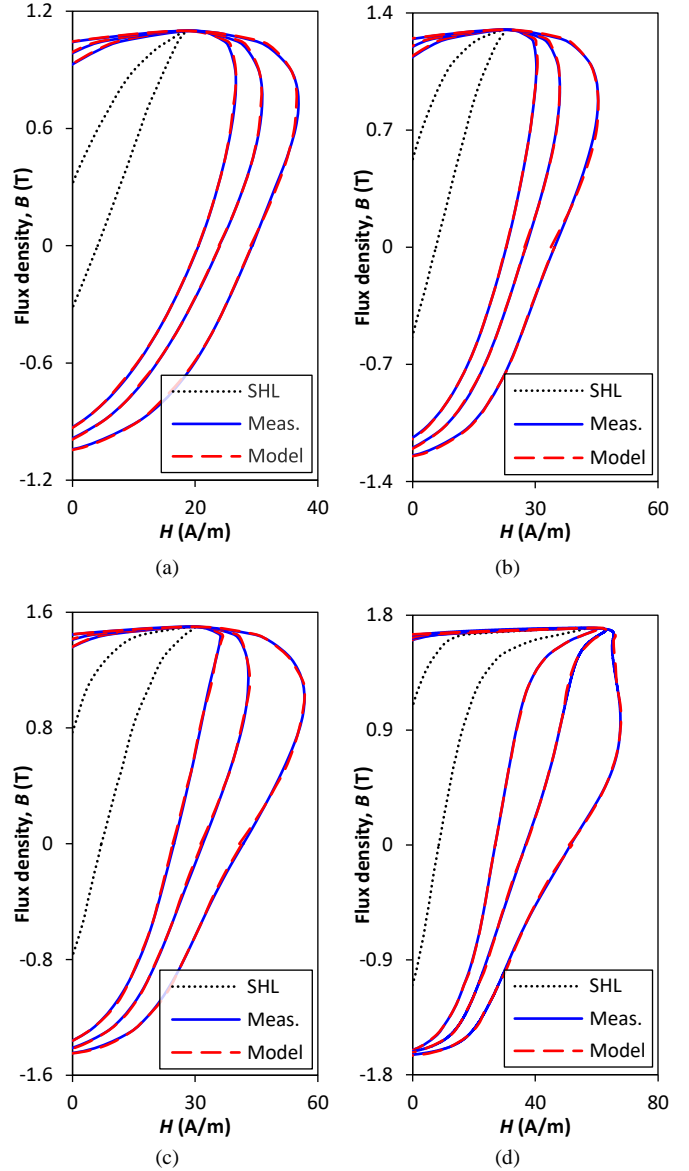

(a)   (b)

(c)   (d)

Fig 7 Measured and modelled dynamic hysteresis loops, $f = 50\,Hz$
(a) $B_{pk} = 1.1\,T$ (b) $B_{pk} = 1.3\,T$ (c) $B_{pk} = 1.5\,T$ and (d) $B_{pk} = 1.7\,T$

Fig 7 shows that the DHLs reproduced from the TSMs (5) and (8) correspond with the measured loops for the range of flux density, which explicitly demonstrate accuracy of the modelling. Furthermore, DHLs of Fig 7 and the instantaneous waveforms of Figs 8 to 11 clearly show how the dynamic behaviour and magnetising processes of magnetic cores are influenced by ILFs. At (B_m, H_b) where $dB/dt = 0$ magnetic flux density changes the direction and, according to the TSM, the dynamic magnetic field $H_{dyn}(t)$ and the additional magnetic field $H_{add}(t)$ are vanished to zero. Therefore, tip of the SHL confluences with the DHL at (B_m, H_b), as shown in Fig 7. It is worth to highlight that at this point, the total magnetic field $H(t)$ is limited to the hysteresis field $H_{hys}(B)$. This phenomenon occurs during each magnetising cycle and can be used as a reliable feature to validate experimental results and analytical modelling of magnetic materials and associated magnetic cores.
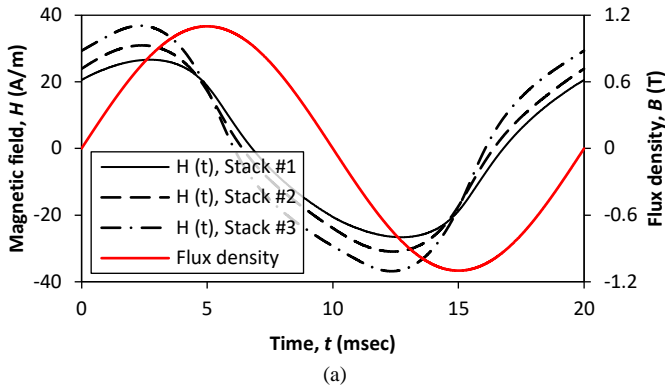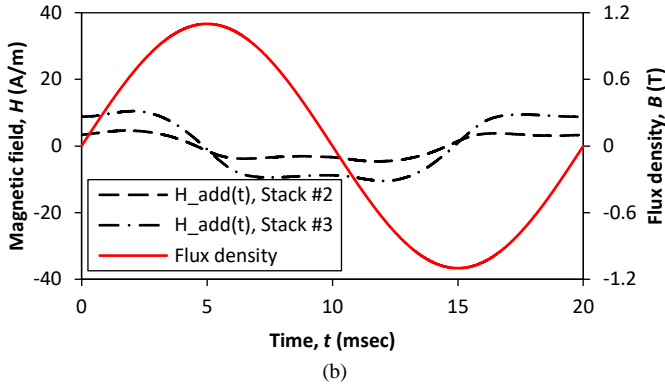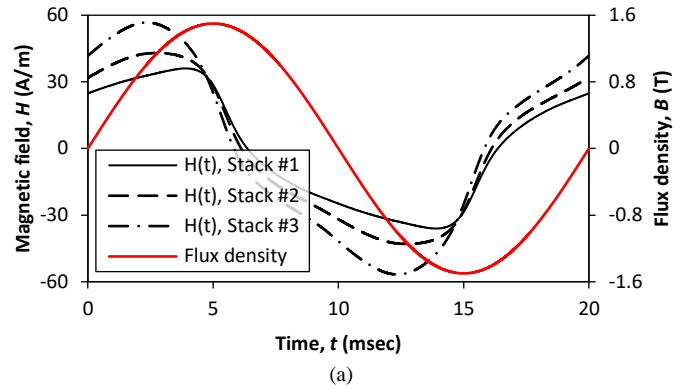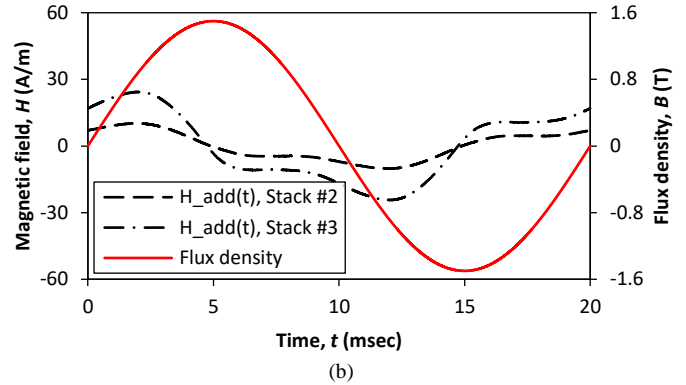
Fig 8 Waveforms of the magnetic fields for one cycle of magnetisation,
$f = 50\ Hz$ and $B_{pk} = 1.1$ T
(a) total magnetic field $H(t)$ (b) additional magnetic field $H_{add}(t)$

Fig 10 Waveforms of the magnetic fields for one cycle of magnetisation,
$f = 50\ Hz$ and $B_{pk} = 1.5$ T
(a) total magnetic field $H(t)$ (b) additional magnetic field $H_{add}(t)$

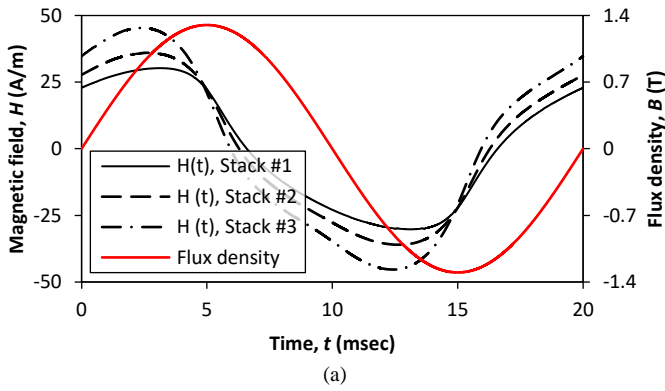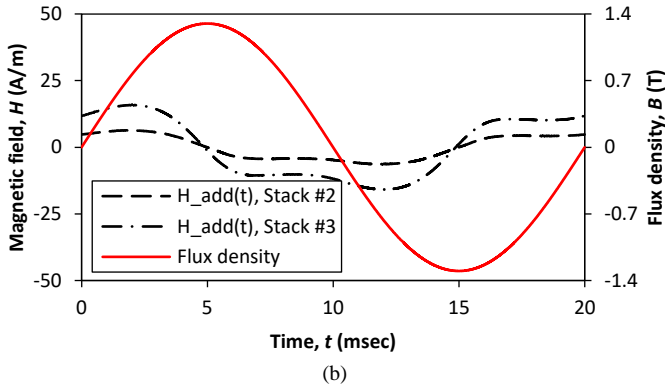Fig 9 Waveforms of the magnetic fields for one cycle of magnetisation,
$f = 50\ Hz$ and $B_{pk} = 1.3$ T
(a) total magnetic field $H(t)$ (b) additional magnetic field $H_{add}(t)$

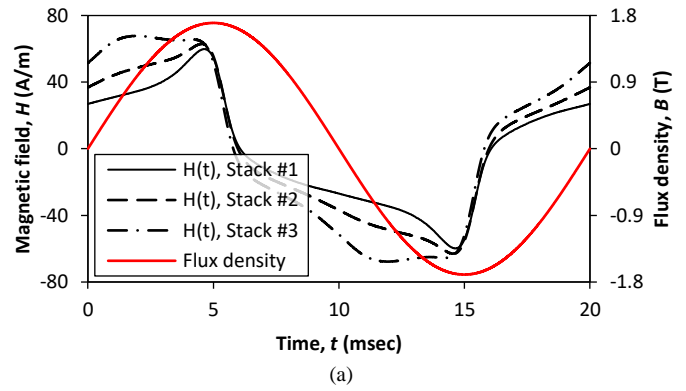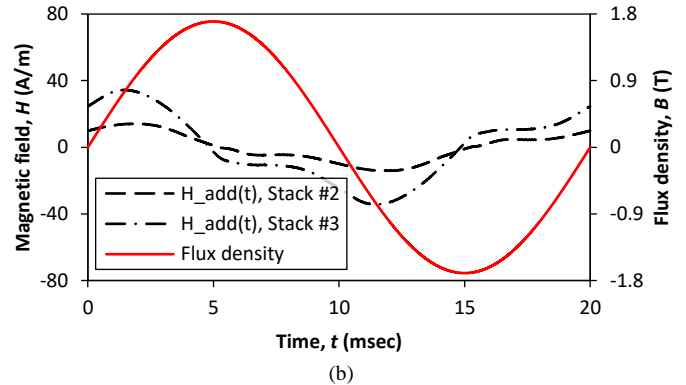Fig 11 Waveforms of the magnetic fields for one cycle of magnetisation,
$f = 50\ Hz$ and $B_{pk} = 1.7$ T
(a) total magnetic field $H(t)$ (b) additional magnetic field $H_{add}(t)$

7

The instantaneous waveforms of Figs 8 to 11, on the other hand, provide additional information about the dynamic behaviour of the test samples and impacts of the ILFs on energy loss mechanism and magnetising processes. Figs 8 to 11 show that, magnetic field strength $H(t)$ of all test samples, including Stack #1 with no ILF, coincide at (B_m, H_b) where $dB/dt = 0$. More importantly at this turning point the additional magnetic field $H_{add}(t)$, and the associated energy loss component W_{add}, for Stack #2 and Stack #3 with ILFs, are vanished to zero. This is further evidenced by the hysteresis loops of Fig 7, where the SHL coincide with the DHL at the same turning point (B_m, H_b). This provides a reliable platform to study impacts of ILFs on quality of the magnetic cores, which eventually help in effective fault diagnosis and condition monitoring of the magnetic cores of practical electromagnetic devices with laminated cores.

Accuracy of the two terms TSM (5) to reproduce DHL of stacks of laminations subjected to ILFs was validated in a recent publication [20]. Using the three terms TSM (8), however, has a distinct advantage to model the additional magnetic field $H_{add}(t)$ due to the ILFs, which consequently help to calculate the associated additional energy loss W_{add}. Following this analysis, total energy loss W_{tot} and dynamic energy loss W_{dyn} of the test samples, and additional energy loss W_{add} of Stack #2 and Stack #3 were calculated; the results are shown in Figs 12 and 13, respectively.
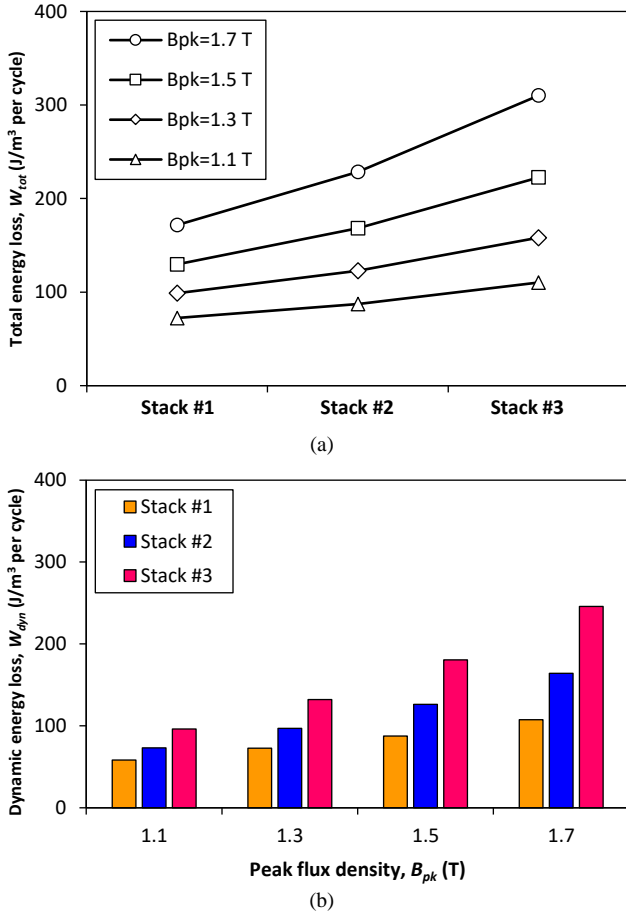

(a)

(b)

Fig 12 (a) Total energy loss, and (b) dynamic energy loss of the test samples, $f = 50\ Hz$, $B_{pk} = 1.1\ T$ to $B_{pk} = 1.7\ T$
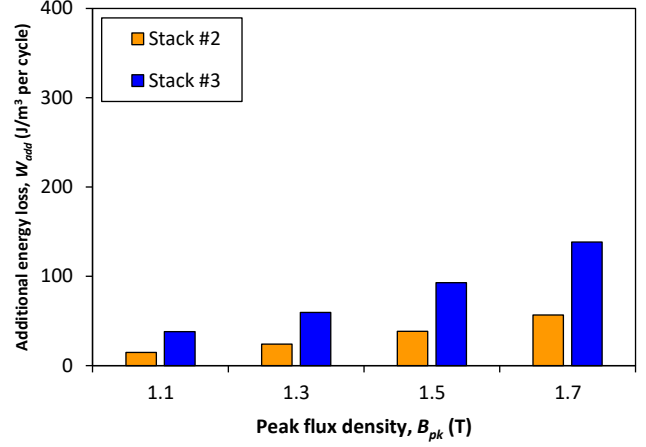

Fig 13 Additional energy loss components of Stack #2 and Stack #3, $f = 50\ Hz$, $B_{pk} = 1.1\ T$ to $B_{pk} = 1.7\ T$

According to Fig 12, dynamic energy loss of Stack #1 at a peak flux density of 1.7 T and magnetizing frequency of 50 Hz accounts for about 62 % of the total energy loss. This complies with the nominal energy loss of 3 wt % SiFe GO steels [22]. However, dynamic energy loss of Stack #2 and Stack #3 is increased to 73 % and 80 % of the total energy loss, respectively. Furthermore, additional energy loss W_{add} of Stack #2 and Stack #3, shows contribution of each ILF in the total energy loss of the test samples. Following decades of research and development in fault diagnosis of magnetic cores, there is now a global agreement that the additional energy loss caused by ILFs is due to the additional eddy current at the defected zone, as shown schematically in Fig 2. Similar to the classical eddy current, this is a rate-dependent phenomenon which occur during each cycle of the magnetisation.

As stated earlier, in industry the main effort is usually on measuring overall power loss of the magnetic cores, known as no-load loss. According to the British standard BS EN 60076-1-2011, no-load loss is "the active power absorbed when a rated voltage (tapping voltage) at a rated frequency is applied to the terminals of one of the windings, the other winding or windings being open circuited" [19]. It is worth to highlight that, such a technique does not necessarily provide a realistic image of quality of the concerned cores, as it only gives the overall power loss, and hence industry is not usually satisfied by the outcomes.

The proposed technique in this paper provides more details on quality of magnetic cores and impacts of core faults on magnetising processes, instantaneous waveshapes of magnetic field strength and its components, DHL, permeability and more importantly additional magnetic field and energy loss. This technique can be further expanded to monitor magnetising process of practical magnetic cores of power transformers, that could be effectively implemented for fault diagnosis and condition monitoring in the product line, as well as during the routine and type tests. For this purpose, in addition to the transformer testing equipment, e.g. power supply, CT and PT, data acquisition system and signal processing unit are required to acquire and process the signals; nevertheless the principle remains the same. A proposed schematic diagram for fault diagnosis of power transformer is shown in Fig 14.
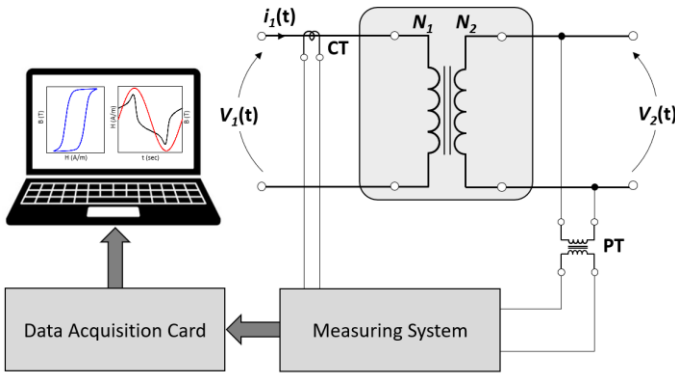
Fig 14 Schematic diagram of fault diagnosis of power transformer

V. LOCALISED POWER LOSS MEASUREMENT

A thermometric measuring system was already developed to monitor localised temperature and power loss of electromagnetic devices [29, 30]. The measuring system implements Type K thermocouple and comprises six independent channels. In this technique, localised power loss is measured by monitoring the initial rate of rise of temperature after magnetisation, and is calculated by [30]:

$$P = c_p \frac{dT(t)}{dt} \quad W/kg \tag{14}$$

where c_p is the specific heat of the material, which is $c_p = 485.6\,J/kg°C$ for GO electrical steels [29]. More details of the measuring system can be found in [29, 30].

In the last part of this work localised power loss of the test samples was measured. For this purpose, the thermocouples were positioned on the surface of the test samples, 3 mm from the edge of the laminations, using double side thermal adhesive tape. The test samples were magnetised using the SST under adiabatic condition, and temperature rise was monitored and recorded in separate databases. Finally, the initial slope of the temperature-time curve was calculated using the linear trend-line in Excel and consequently localised power loss was calculated according to (14). A MATLAB code was developed based on the *meshgrid* function, a powerful feature of MATLAB, to transfer the localised power loss on a 3D colour surface. This function plots the localised power loss values in a *z*-matrix above the grid surface defined by *x* and *y* matrixes. The 3D colour surface varies according to the localised power loss values defined by the *z*-matrix. The results for Stacks #2 and #3 are shown in Figs 15 and 16, respectively.

Figures 15 and 16 indicate a significant increase in localised power loss near the defective zone. The experimental results of Stack #2 showed that, localised power loss at the centre of the fault current loop rose to 5 W/kg at a peak flux density of 1.7 T, while power loss at the healthy zones is $0.68\,W/kg$ at the same flux density. Looking at the schematic diagram of Fig 2, current density at the defective zones is much higher than other parts of the test sample. This implies that the local power loss near the artificial fault, or edge burr in real magnetic cores, is much higher than other parts; localised measurements of Figs 15 and 16 explicitly demonstrate this.
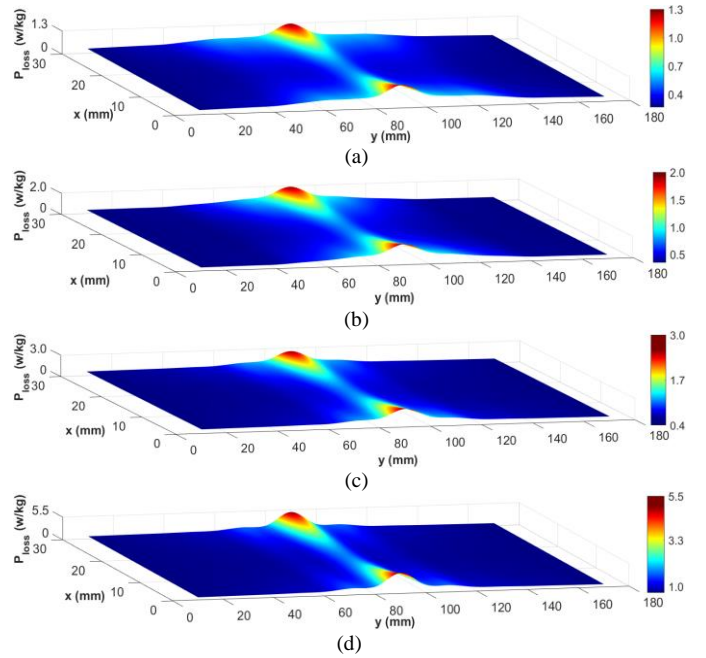

(a)

(b)

(c)

(d)

Fig 15 3-D distribution of localised power loss of Stack #2 at $f = 50\,Hz$
(a) $B_{pk} = 1.1\,T$ (b) $B_{pk} = 1.3\,T$ (c) $B_{pk} = 1.5\,T$ and (d) $B_{pk} = 1.7\,T$
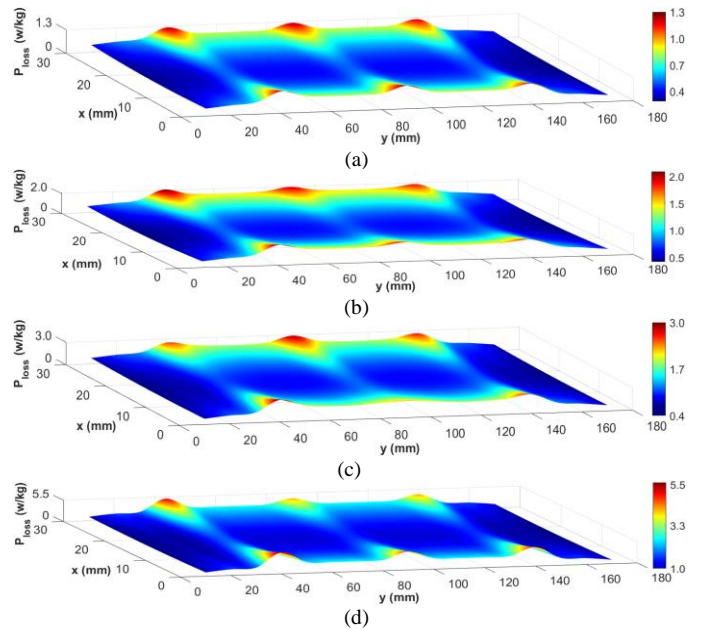

(a)

(b)

(c)

(d)

Fig 16 3-D distribution of localised power loss of Stack #3 at $f = 50\,Hz$
(a) $B_{pk} = 1.1\,T$ (b) $B_{pk} = 1.3\,T$ (c) $B_{pk} = 1.5\,T$ and (d) $B_{pk} = 1.7\,T$

VI. CONCLUSION

There is a growing recognition that ILF problems and their consequences pose serious threats on the normal operation of the magnetic cores. Despite the long history of the ILFs problem, research and development are still underway within the academic and industrial communities for further understanding their impacts on electric and magnetic properties of magnetic materials and magnetic cores. This not only helps to understand and analyse the core fault problems but provides a practical platform to safeguard the magnetic cores against them.

Following a series of research conducted by the author, it was experimentally and analytically shown that phenomenology of the magnetic hysteresis is a reliable approach for fault diagnosis and condition monitoring of magnetic cores. This paper continued the previous work with the specific emphasis on the additional magnetic field and energy loss caused by ILFs. For this purpose, experimental work and analytical modelling were performed on stacks of Epstein size laminations, subjected to different types of artificial faults. Dynamic characteristics of the test samples, including DHLs and instantaneous waveforms of the magnetic field strength, were measured using a standard SST. An analytical model, based on the TSM, was then developed to analyse impacts of the ILFs on dynamic characteristics of the test samples. The distinct feature of the developed model is its ability to calculate the additional magnetic field caused by ILFs, and the associated energy loss.

This study demonstrated that monitoring the DHLs and an in-depth analysis on the magnetising processes are effective techniques in fault diagnosis and condition monitoring of magnetic cores. In fact, the developed analytical model and in particular the additional term of magnetic field can be applied to calculate the additional eddy current loss in the defected zone. This can be implemented by the design engineers at the design stage to quantify eddy current distribution in practical magnetic cores. Furthermore, this can be used in effective condition monitoring of of practical power transformers during the routine and type tests. A thermometric method was also used to measure localised power loss of the test samples at and around the defective zone of the test samples. The results highlighted that localised power loss at the defective zone could reach up to about 6 times higher than the nominal loss of the materials.

More analytical and experimental studies on fault diagnosis and condition monitoring of magnetic cores have been planned as future work. In this respect, the author in corporation with other researchers, is working on two area of research: 3D FE modelling to visualise eddy current and magnetic field distribution at the defected zone, and spectrum analysis of magnetic field strength. This study and the relevant FE modelling are built based on the analytical approach proposed in this paper, and the additional term of magnetic field strength caused by the ILFs. Furthermore, implementing the proposed technique to practical magnetic cores of power transformers and rotating machines will be considered as long-term research plan.

REFERENCES

[1] S Athikessavan, E Jeyasankar, S Manohar and S Panda, "Inter-Turn Fault Detection of Dry-Type Transformers Using Core-Leakage Fluxes," in IEEE Transactions on Power Delivery, Vol. 34, No. 4, pp. 1230-1241, Aug. 2019

[2] Y Akhmetov, V Nurmanova, M Bagheri, A Zollanvari and G Gharehpetian, "A Bootstrapping Solution for Effective Interpretation of Transformer Winding Frequency Response," IEEE Transactions on Instrumentation and Measurement, Vol. 71, pp. 1-11, 2022, Art no. 3508811

[3] P Zhang and D Lu, "A Survey of Condition Monitoring and Fault Diagnosis toward Integrated O&M for Wind Turbines," Energies, vol. 12, no. 14, p. 2801, Jul. 2019

[4] IEEE Std. C37.91, 2000 IEEE "Guide for Protective Relay Applications to Power Transformers", 2000

[5] Z Tang, X Zhang, L Wan, Y Ouyang, Z Gao, Q Wei, A Wang, H Yang, Y Wu, Y Zhang, H Wang and H Wang, "Blue Laser Welding of Laminated Electrical Steels: Dynamic Process, Weld Bead Characteristics, Mechanical and Magnetic Properties", Journal of Materials Processing Technology, Vol 312, 2023, 117859

[6] M Bali and A Muetze, "Modelling the Effect of Cutting on the Magnetic Properties of Electrical Steel Sheets," in IEEE Transactions on Industrial Electronics, vol. 64, no. 3, pp. 2547-2556, March 2017

[7] K Bourchas, A Stening, J Soulard, A Broddefalk, M Lindenmo, M Dahlen, and F Gyllensten, "Quantifying Effects of Cutting and Welding on Magnetic Properties of Electrical Steels", IEEE Transactions on Industry Applications, Vol. 53, No. 5, pp. 4269-4278, Sept.-Oct. 2017

[8] S Shah, O Osemwinyen, P Rasilo, A Belahcen, A Arkkio, "Thermographic Measurement and Simulation of Power Losses Due to Interlaminar Contacts in Electrical Sheets", IEEE Transactions on Instrumentation and Measurement, Vol. 67, No. 11, pp. 2628-2634, 2018

[9] D Bertenshaw, C Ho, A Smith, M Sasi, and T Chan, "Electromagnetic modelling and detection of buried stator core faults", IET Electric Power Applications, Vol. 11, Issue 2, March 2017, pp. 187–196

[10] H Hamzehbahmani, "A Phenomenological Approach for Condition Monitoring of Magnetic Cores Based on the Hysteresis Phenomenon," IEEE Trans. on Instru. and Meas., Vol. 70, pp. 1-9, December 2020

[11] G Bazan , A Goedtel , P Scalassara, W Endo , E Nunes , V Takase, J Guedes, and M Gentil, "An Embedded System for Stator Short-Circuit Diagnosis in Three-Phase Induction Motors Using Information Theory and Artificial Neural Networks," IEEE Transactions on Systems, Man, and Cybernetics: Systems, Vol. 52, No. 10, pp. 6582-6592, Oct. 2022

[12] M-Q Tran, M-K. Liu, Q-V. Tran and T-K. Nguyen, "Effective Fault Diagnosis Based on Wavelet and Convolutional Attention Neural Network for Induction Motors," IEEE Transactions on Instrumentation and Measurement, Vol. 71, pp. 1-13, 2022, Art no. 3501613

[13] K Lee, J Hong, K Lee, S B Lee and E J Wiedenbrug, "A Stator Core Quality Assessment Technique for Inverter-fed Induction Machines", IEEE Industry Applications Society Annual Meeting, Oct 2008, pp 1-8

[14] G Kliman, S Lee, M Shah, R Lusted, and N Nair, "A new method for synchronous generator core quality evaluation," IEEE Trans. Energy Convers., Vol. 19, NO. 3, Sep. 2004, pp. 576–582

[15] H Hamzehbahmani, P Anderson, K Jenkins "Inter-laminar Insulation Faults Detection and Quality Assessment of Magnetic Cores Using Flux Injection Probe", IEEE Trans on Power Del, Vol. 30, No. 5, Oct 2015, pp. 2205-2214

[16] C Huo, Y Wang, S Wu and C Liu, "Research on Residual Flux Density Measurement for Single-Phase Transformer Core Based on Energy Changes," IEEE Transactions on Instrumentation and Measurement, Vol. 70, pp. 1-9, 2021, Art no. 6011909

[17] V Gurusamy, G-A. Capolino, B Akin, H Henao, R Romary and R Pusca, "Recent Trends in Magnetic Sensors and Flux-Based Condition Monitoring of Electromagnetic Devices," IEEE Transactions on Industry Applications, Vol. 58, no. 4, pp. 4668-4684, July-Aug. 2022

[18] S Nguedjang Kouakeuo , A Solignac , R Sabariego , L Morel, M-A Raulet, B Toutsop, P Tsafack, and B Ducharne, "Internal Characterization of Magnetic Cores, Comparison to Finite Element Simulations: A Route for Dimensioning and Condition Monitoring," IEEE Transactions on Instrumentation and Measurement, Vol. 71, pp. 1-10, 2022, Art no. 6005310

[19] BS EN 60076-1-2011, Power transformers - Part 1: General, British Standard, 2012

[20] H Hamzehbahmani, "An Experimental Approach for Condition Monitoring of Magnetic Cores with Grain Oriented Electrical Steels", IEEE Trans. on Instru. and Meas., Vol. 69, No. 6, June 2020, pp. 3395-3402

[21] H Hamzehbahmani, "Development of a New Approach to Core Quality Assessment of Modern Electrical Machines", IET Electric Power Applications, Vol. 13, Issue 6, June 2019, pp. 750–756

[22] G Bertotti, "General properties of power losses in soft ferromagnetic materials," in IEEE Trans. on Magn., Vol. 24, no. 1, pp. 621-630, Jan. 1988

[23] S Zirka, Y Moroz, P Marketos, A Moses and D Jiles "Measurement and modeling of B-H loops and losses of high silicon non-oriented steels", IEEE Trans. Magn., Vol. 42, No. 10, pp. 3177-3179, 2006

[24] S Zirka, Y Moroz, S Steentjes, K Hameyer, K Chwastek, S Zurek and R Harrison "Dynamic magnetization models for soft ferromagnetic materials with coarse and fine domain structures", Journal of Magnetism and Magnetic Materials, Vol. 394, pp 229-236, Nov. 2015

[25] S Zirka, Y Moroz, P Marketos, A Moses, D Jiles and T Matsuo, "Generalization of the Classical Method for Calculating Dynamic Hysteresis Loops in Grain-Oriented Electrical Steels," in IEEE Transactions on Magnetics, vol. 44, no. 9, pp. 2113-2126, Sept. 2008

[26] BS EN 10280:2001 + A1:2007, Magnetic Materials - Methods of measurement of the magnetic properties of electrical sheet and strip by means of a single sheet tester, British Standard, 2007

[27] UKAS M3003, "The Expression of Uncertainty and Confidence in Measurement", Edition 4, Oct 2019

[28] H Hamzehbahmani, "Static Hysteresis Modelling for Grain-Oriented Electrical Steels based on the Phenomenological Concepts of Energy Loss Mechanism", Journal of Applied Physics, Vol. 130, Issue 5, August 2021

[29] H Hamzehbahmani, A Moses and F Anayi "Opportunities and Precautions in Measurement of Power Loss in Electrical Steel Laminations Using the Initial Rate of Rise of Temperature Method" IEEE Trans. Mag. Vol. 49, No. 3, March 2013, pp 1264- 1273

[30] R Mazurek, H Hamzehbahmani, A Moses, P Anderson, F Anayi and T Belgrand, "Effect of Artificial Burrs on Local Power Loss in a Three-Phase Transformer" IEEE Trans. Mag. Vol. 48, No. 4, April 2012, pp 1653-1656

BIOGRAPHY

Hamed Hamzehbahmani (SM' 18) received the BEng and MSc degrees in electrical engineering in 2005 and 2007, respectively; and PhD degree in electrical engineering from Cardiff University, UK in 2014. Between 2005 and 2010 he worked on distribution networks and HV substations as a consultant engineer. Following his PhD he was appointed as a research associate at Cardiff University in the field of earthing systems for HVAC and HVDC systems, in corporation with UK National Grid. From 2016 to 2018 he was a lecturer in electrical engineering with Ulster University in UK. He is currently an assistant professor in electrical engineering at Durham University in the UK. His main research interests include magnetic materials and applications, static and dynamic modelling of magnetic materials, power loss analysis and condition monitoring of power transformers and electrical machines, high frequency and transient response analysis of earthing systems, earthing design of HVAC and HVDC networks.

Dr Hamzehbahmani is a Chartered Engineer, Member of IET, Senior Member of IEEE, and Fellow of the Higher Education Academy. He is also associate editor of IEEE Transactions on Instrumentation and Measurement.